Recent Evolution of the Sub-Catalogue Space Debris Population in High-altitude Orbital Regions

Thomas Schildknecht, Fiona Pärli, Alessandro Vananti, Palash Patole, Peter Pessev
Astronomical Institute, University of Bern, Sidlerstr. 5, CH-3012 Bern, Switzerland
Tim Flohrer, Jan Siminski
Space Debris Office, ESA/ESOC, Germany

ABSTRACT

The Astronomical Institute of the University of Bern (AIUB) performs optical surveys for sub-catalogue space debris in high-altitude orbits since more than two decades. The bulk of the data is acquired on behalf of ESA with the ESA 1-meter telescope at the Optical Ground Station (OGS) in Tenerife, Spain. Additional surveys are performed with the 0.8-meter Zimmerwald Multiple Applications Telescope ZimMAIN at AIUB's Zimmerwald Observatory in Switzerland.

Continuous observation campaigns are key to monitor this environment for new sources of space debris. Results from the last 5 years indicate the appearance of several new clusters of fragments and emphasize the dynamical nature of this environment. Preliminary findings of a larger effort to consistently re-process the data of 22 years of surveys, analyse possible observational selection effects, and to compare the actual observations with reference populations, in particular the MASTER population, will be presented.

1. INTRODUCTION

ESA has recognized the paramount importance of protecting the geostationary ring from contaminating space debris long time ago [1], [2], [3]. It was and is evident that the search for fragments in the geostationary ring and a better knowledge of the debris population in GEO are required to understand the future evolution of the debris population, to assess the collision risk and to define suitable and cost-efficient mitigation measures. Consequently, ESA initiated around 1990 a program to establish optical debris searches in GEO and high-altitude regions [4].

The main sensor of ESA's optical survey program to investigate and monitor the space debris population in high-altitude orbits is the ESA 1-meter telescope at the OGS in Tenerife, Spain (Figure 1). During the 90ies of the last century the sensor was deployed together with a dedicated space debris camera. The necessary planning, data acquisition, and data processing software was developed at the same time by AIUB on behalf of ESA. Both, the camera hardware and the software components experienced a major upgrade over the past 25 years. In 1999 the optical survey program became operational. After an interruption due to hardware issues the surveys program is continuously executed since 2001.

Figure 1: ESA 1-meter telescope at the Optical Ground Station (OGS) in Tenerife, Spain.

The main objective of these surveys is to derive statistical data on the small-size debris population in the GEO and GTO region as input for the ESA Meteoroid And Space debris Terrestrial Environment Reference (MASTER) population model [5]. As the field of view of the ESA telescope is only 0.7°, objects detected in the surveys appear on two to three consecutive frames only. These short series of observations, also called tracklets, are spanning an arc of about one to two minutes and thus do not allow for a full 6-parameter orbit determination. The inferred circular orbits might be valid for a part of the population in the GEO region but not for objects in GTO. It was thus decided to follow-up a small subset of these "detections" and acquire additional observations with the aim to determine 6-parameter orbits.

Even the very first observations revealed a hitherto unknown population of small-size debris in high-altitude orbits in and near GEO (all observations were correlated with the publicly available data from USSTRATCOM). Figure 2 shows the magnitude distribution for the objects discovered during the time period from June 2002 to December 2006. The indicated object sizes were derived by assuming Lambertian scattering spheres and an albedo of 0.1. There is a steep rise in terms of numbers for objects smaller than about 1m with a peak at about 20cm diameter. It is important to note that the decrease in the number of objects fainter than magnitude 19 is entirely due to the limiting magnitude of the observation system.

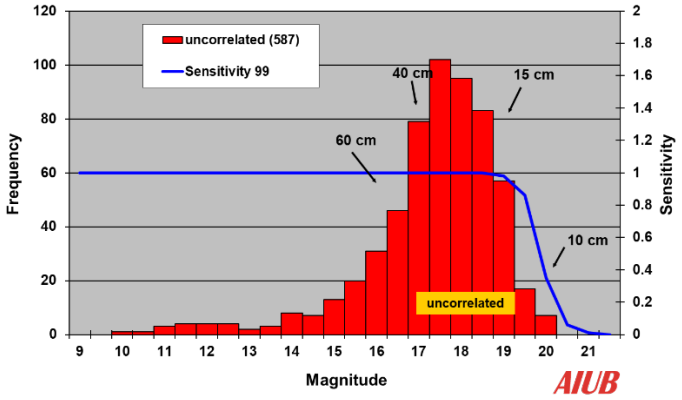

Figure 2: Magnitude distribution for the objects discovered during the time period from June 2002 to December 2006 (only objects for which elliptical orbits could be determined). The indicated object sizes were derived by assuming Lambertian scattering spheres and an albedo of 0.1. The solid line shows the instrument sensitivity as determined from independent calibration observations.

From these observations it became clear, that the majority of the newly discovered objects must be fragments either released from intact spacecraft due to aging processes or produced during breakup events. The results from these surveys were used as input to improve the MASTER model.

The aim of this paper is to compare the observations from 22 years of surveys from the ESA telescope with simulated observations based on the MASTER model population. The additional surveys performed with the ZimMAIN telescope at AIUB's Zimmerwald Observatory in Switzerland were not used for this comparison. Note that follow-up observations from the Zimmerwald Observatory were used to determine 6-parameter orbit for a subset of the objects discovered in the ESA telescope.

2. OBSERVATION SCENARIOS

The survey observations are scheduled for 4 to 10 nights during 6-12 months per year around the New Moon periods. The surveys are performed using series of observations of the same star field. During the exposures, however, the telescope is in 'staring mode', i.e., not tracking the stars, but tracking with the expected velocity of the objects of interest. The exposure time is set to 2 seconds limiting the area covered by star trails to less than 7%. It is reasonable to adopt the hypothesis that the catalogued GEO objects trace the debris population, and the fields for the GEO surveys are thus selected to cover the orbital planes of the catalogue population. For more details on the survey technique see [6].

The fields intended to discover objects in low inclination ($i < 25°$) GTO orbits are place such that the apogee regions of these orbits were covered. Tracking during the exposures is optimized for the apparent velocity of objects in GTO orbits.

All observations are processed in real time at the OGS. For all uncorrelated discoveries near real-time follow-up observations are performed during the discovery night to derive full 6-parameter orbits ("elliptical orbits"). If the follow-up observations are successful, these objects are handed over to the AIUB sensors to maintain their orbits. Full orbits are

derived for only about 20% of the discoveries. In most cases the first near-real-time follow-up observation is failing to rediscover the object, although about 30% of the telescope time is spent for such observations. The majority of these objects is lost after a few days or weeks due to insufficient tracking and considerable non-gravitational perturbations of their orbits. Nevertheless, the small population of objects with 6-parameter orbits may be assumed to trace the full population of debris objects as the decision to initiate a follow up is agnostic to any orbital characteristics (apart from being in a high-altitude orbit with an apogee higher than about 25'000km altitude). It may in particular be used as a "ground truth" to be compared to the "detections" with inferred circular orbits. Comparing orbital characteristics of 6-parameter orbits with the inferred circular orbits is only possible to a limited extent and under certain assumptions. If we assume that the objects in elliptical orbits are detected preferentially at their apogee, as the surveys are designed for, we may conclude that the orientation of the orbital planes as inferred from the circular orbit determination is representing the true orientation of their orbital planes to a good extent.

Figure 3 shows the orientation of the orbital planes (inclination i as a function of the right ascension of the ascending node Ω) for the detections and the objects with 6-parameter orbits for the year 2005. The main feature in the figure of the detections is due to precession of the orbital planes of uncontrolled objects in the GEO region. In fact, the orbital plane of an uncontrolled object in the GEO will precess around the so-called Laplacian plane with a period of about 53 years due to gravitational perturbations. This feature is also seen in the 6-parameter orbits. In addition, the orbital planes of the detections show several concentrations ("clusters"), e.g., at (-20°/11°) and (10°/14°). Some minor concentrations at the same places can also be seen in the 6-paramer orbits. "Clusters" in the orientation of the orbital planes are indicative of fragmentation events. Orbital planes of the 6-parameter orbits which are not aligned along the evolution paths due to the precession around the Laplacian plane are in fact related to eccentric orbits, mostly GTO orbits. We may infer that the same holds for the scattered orbital planes in the figure with the detections. However, in general we cannot assume that a circular orbit determination will result in the correct orientation of the orbital plane for elliptical orbits, except for objects which were observed near the apogee. As the surveys are designed to observe GTO objects near the apogee, probably most of the determined orbital planes for the detections are near the real ones, even for elliptical orbits.

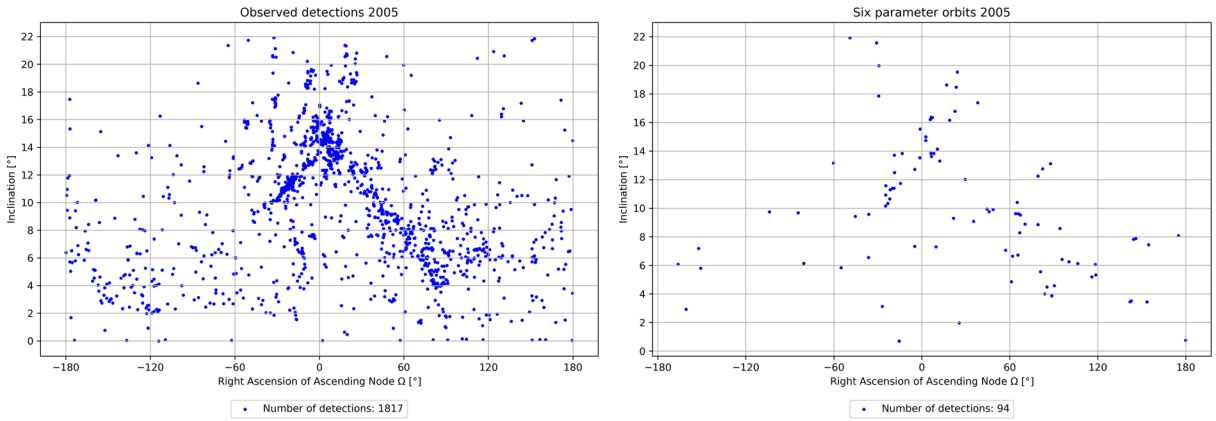

Figure 3: Orientation of the orbital planes for the detections (left) and the objects with 6-parameter orbits (right) for the year 2005.

3. SIMULATED OBSERVATIONS BASED ON MASTER MODEL

A primary objective was to compare the observations with the ESA MASTER model [10]. To process the data from the MASTER model, the Program for Radar and Optical Observation Forecasting (PROOF) software from ESA was used. PROOF serves to validate space debris models – in this case the ESA MASTER model. It provides mathematical methods to determine crossing rates for given observation scenarios and translating these into detection rates, based on the provided sensor model. PROOF yields the properties of the crossing and detection objects, including orbital parameters, size and magnitude.

The ESA MASTER is designed to model the natural and human-made near-earth environment and evaluate the impact of space debris on missions. The model is composed of different models of each space debris source term, namely collision and explosion fragments, mission related objects, NaK droplets, SRM slag and dust, paint flakes, ejecta, multi-layer insulation (MLI) and meteoroids [13]. While the MASTER model itself contains a probability flux and spatial density

prediction, it features an additional tool containing resolved objects, which serve as an input for the simulations using PROOF. These population files were applied on a yearly basis to the simulations, note that the latest population file available dates to November 2016, all simulations for data collected later were performed with this version of the MASTER model.

PROOF was set to the statistical mode, the so-called "Resolution of the Sampling Factor" was enabled, this forces the software to resolve the data from the population files into individual objects, as the population files contain representative objects, meaning one object represents several real objects with similar sizes and orbital parameters. Small objects, which are exponentially more numerous, are likely to have a higher representation factor, which makes the simulation more efficient when including small debris. As our lower diameter threshold is quite large and the aim is to compare the number of simulated detections to the observed ones, enabling the Resolution of Sampling Factor is of crucial importance [12].

The input for PROOF consists mainly of two components, which are the description of the optical system and the parameters of the ground-based observation scenario. The description of the optical system consists of parameters such as the diameter of the aperture, the size of the field of view, the number of pixels per row, pixel size, full width of half max as well as integration and gap times. The following parameters are relevant for the detection model: minimum number of consecutive frames (is set to 2 in our case), threshold factor, albedo and the count rate constant for CCD readout noise and for dark noise. PROOF uses a discrete star catalogue, for which a maximum magnitude must be specified, beyond which stars are treated as a continuous source. Additionally, the optical system transmission spectrum and the CCD quantum efficiency spectrum must be provided. For the ground-based scenario description, the coordinates (geodetic latitude, longitude and altitude) of the sensor need to be defined. The coordinates of the line of sight are given in the inertial system. Furthermore, the tracking angular velocity, maximum and minimum range, the coordinates of the tracking pole and of the array normal direction and the scanning period need to be indicated.

Besides the specification of the sensor and telescope, PROOF was provided by the yearly automation files. The automation mode allows efficient processing of sub campaigns, which only differ by a small number of parameters. The automation mode offers to process the data in yearly batches, which also leads the output to be in annual packets. In our case, the automation files consisted of the detailed observation time, coordinates of the line of sight, tracking angular velocity, integration and gap times of the observations that were executed in Tenerife. PROOF performs simulation for the exact parameters of the observation which ensures comparability between simulated and observed data.

After correlating the magnitudes and the sizes of the simulation results using a minimum diameter threshold of 5 cm, it was clear that the brightness of small objects was most likely below the detection threshold, so the lower diameter threshold was set to 10cm. This drastically reduced the CPU time. It should be noted that the diameter cutoff is entirely artificial, as the number of objects grows exponentially with decreasing size.

Each space object incorporated into the MASTER model has a source term associated to it. When limiting the analysis to objects larger than 10 cm, the vast majority of all objects are either TLEs (correlated), fragments or Multi-Layer-Insulation objects. For the comparison with the uncorrelated observations, the TLEs were excluded from the outputs for all further analysis.

The observation scenarios for the telescope in Tenerife are designed to either target for GEO or GTO objects, with the GEO survey focusing on different fields of view than the GTO survey. In addition, the tracking rates during the exposures were different for the two scenarios. For some uncorrelated objects follow-up observations were performed. The survey type (GEO, GTO or Follow-up) is specified in the automation file for each survey field. Thus, the output was categorized into these three orbit types (technically, Follow-up is not an orbit type, but is referred as such for simplicity). The division of the results in the orbit types may allow to assess the effectiveness of the survey designs. For each yearly data batch and for each orbit type, there were four PROOF runs performed, each with a different random seed, providing more statistical robustness. This will allow us to investigate the accuracy of results.

The PROOF output consists of a crossing and a detection file. Both files contain a list of objects with several attributes such as orbital parameters, magnitudes, the source term and more. In both, the simulations and observations an object can be detected multiple times. PROOF assigns each object an identifier number, valid locally within that run, which enables us to find the number of unique detections within a single run. However, when comparing detections from different runs (meaning different years or different orbit types), it is no longer possible to identify objects that were detected multiple times only using the enumeration of the objects by PROOF. Therefore, an algorithm to find unique detections was constructed, which finds unique objects based on their attributes. The algorithm decides based on a list of tolerances for each attribute whether two detections belong to the same object. The tolerance list was tuned by applying the algorithm to data sets resulting from single runs and comparing its number of non- duplicate objects to the sorting based on the identifier numbers assigned by PROOF.

From now on, the term “object” denotes the actual number of objects. In the other hand, the term “detections” refers to the observed instances, regardless of the fact that some of these detections might be the same object [15].

To improve statistical significance, the results were grouped into 4-year batches. The detections were filtered in the following way: All objects with inclinations higher than i = 22° were removed as these are likely not GEO objects and therefore not of primary interest in this study. In addition, all TLE objects were removed to make the simulations comparable to the uncorrelated detections. As some detections were found to have an apparent magnitude of zero, it was concluded that they were most likely in the earth shadow and PROOF had misleadingly still incorporated them into the simulation. When removing all objects with an apogee lower than 10’000 km, the issue was resolved and the hypothesis that these objects were in the earth shadow was confirmed.

When comparing the magnitudes of the observed detections to the magnitudes of the simulated detections, there was a significant discrepancy, as there was a local maximum in the observations at around 11 to 13 magnitudes, which was absent in the simulations. This is likely due to a deficiency on the correlation algorithm used in the real-time processing at the observatory in Tenerife. After trying to move the detections that were TLEs from the GTO survey or moving the detections that were TLEs in GTO based on their semi-major axis to the simulated detections, it was not possible to properly remove the discrepancy for unclear reasons. Therefore, it was decided to remove all objects from the data with a magnitude brighter than 14.5 mag, as there are most probably TLEs and not debris.

4. COMPARISON OF THE OBSERVED EVOLUTION OF THE SPACE DEBRIS POPULATION WITH THE MASTER MODEL

Changes in the space debris population may be characterized by analyzing different characteristics. Obviously, the evolution of the number of debris, e.g., as a function of debris size, in particular orbital regions is of interest. Extrapolating the total number of objects from the detections within the surveys is challenging for two reasons: a) the average number of detections per object within a particular survey, e.g., over one year needs to be assessed, and b) the overall coverage of the population by the surveys needs to be determined. Both quantities depend on the assumed distribution of the orbital elements of a “reference population”. The latter is, however, unknown and could only be established by adjusting the MASTER model in an iterative process. This has not been done so far. Even comparing the number of observed detections with the number of simulated detections is not directly possible, as the simulations depend on subtle details of the sensor model. Figure 4 shows the distribution of apparent magnitudes for the observation data (detections, left) and the simulated detections (right). The distribution of the real observations starts to fall off for magnitudes fainter 18.5 while for the simulations the number of detections is only decreasing for magnitudes fainter than 19. Moreover, the fall-off is steeper for the simulations than for the real observations. Obviously, the sensor model is too optimistic for the limiting magnitude of the real data and will have to be further tuned accordingly.

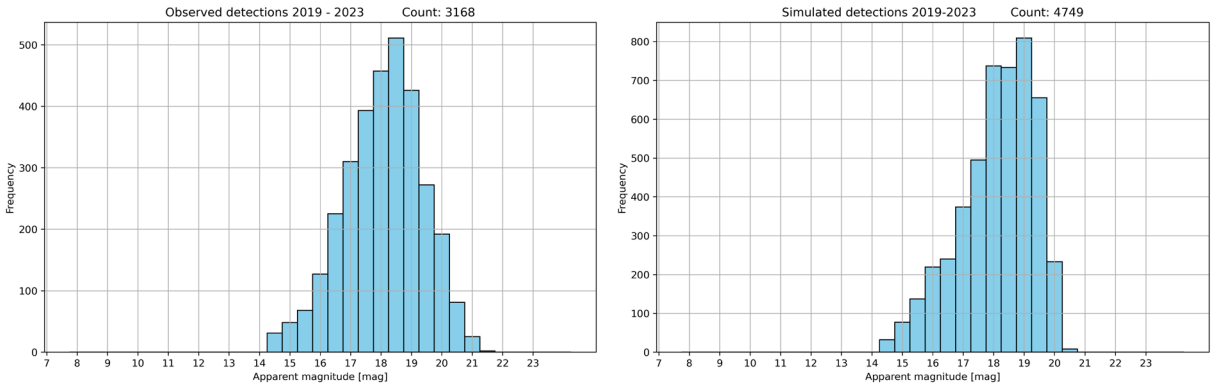

Figure 4: Distribution of apparent magnitudes for the observation data (detections, left) and the simulated data (detections, right) for the time period 2019 – 2023. Note that the detections brighter than magnitude 14.5 were excluded.

Another characteristic of the population is the distribution of the orbital planes which may be analyzed and compared for the observations and the simulations without knowing the total numbers of objects or the exact details about the limits at the faint end of the magnitude distribution. The distribution of the orientation of the orbital planes may reveal classes of orbits and in particular fragmentation debris clouds which will show up as “concentrations” in a corresponding diagram. For the following analysis all simulated and all real observations were binned into 4-year periods in order provide more statistical significance.

Figure 5, Figure 6, Figure 7, Figure 8, and Figure 9 show the orientation of the orbital planes of observed detections (top left), simulated detections (top right), and 6-parameter orbits (bottom) for the different time periods. Colors indicate in which observation scenarios the detections occurred (GEO, GTO of Follow-up), both, for the real observations and the simulations. Note that the “detections” in the follow-up scenarios are new discoveries which occurred in the follow-up observations and do not relate to the objects which were followed up.

Period 2001 to 2005 (Figure 5)

Comparing the detections with the simulations reveals that the main observed clusters along the "evolution path" are well modeled by MASTER. To a certain extent this is not surprising, as the MASTER model was based on some of the observation data as input for its validation. On the other hand, the simulations predict observations of a cluster along the line (-130°/3°, -90°/6°) were there are no detections. Either this cluster did not exist, or it evolved differently than predicted by MASTER. This could be the case if, e.g., most of the fragments in this cluster were high area-to-mass (HAMR) objects resulting in a dispersion of the cluster over time due to perturbations of the orbital planes by solar radiation pressure. The figures of the 6-parameter orbits and the detections show both a cluster in the region (30°/8°, 120°/6°) where MASTER does not predict a concentration. The simulated observations show prominent horizontal "lines" in the range from 4° to 8° inclination which are fragments attributed to Ariane GTO upper stages launched from Kourou. As there are no significant concentrations in the detections for this range the conclusion is that either MASTER is overestimating this population or that the sensor model in PROOF is too optimistic for the GTO survey scenarios. This will need to be further analyzed.

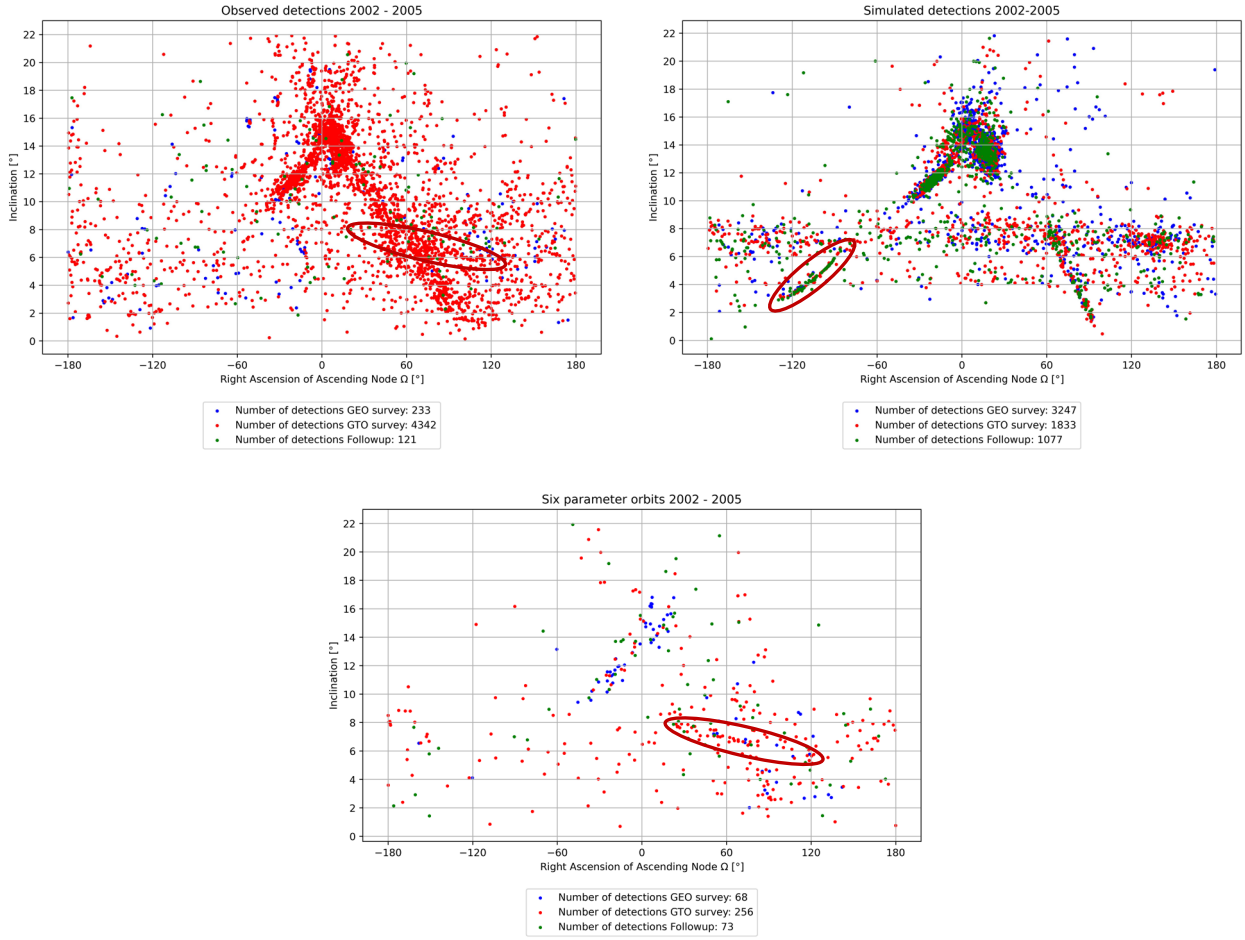

Figure 5: Orientation of the orbital planes of observed detections (top left), simulated detections (top right), and 6-parameter orbits (bottom) for the period 2001 to 2005.

Period 2006 to 2009 (Figure 6)

The main clusters along the "evolution path" are essentially seen in the detections and the 6-parameter orbits as predicted by the simulations. Again, the predicted GTO fragments are not seen as in the previous period. The cluster along the line (120°/3°, 180°/2°) - (-180°/2°, -120°/4°) in the simulated observations, actually the same cluster as in the previous period, is again not observed.

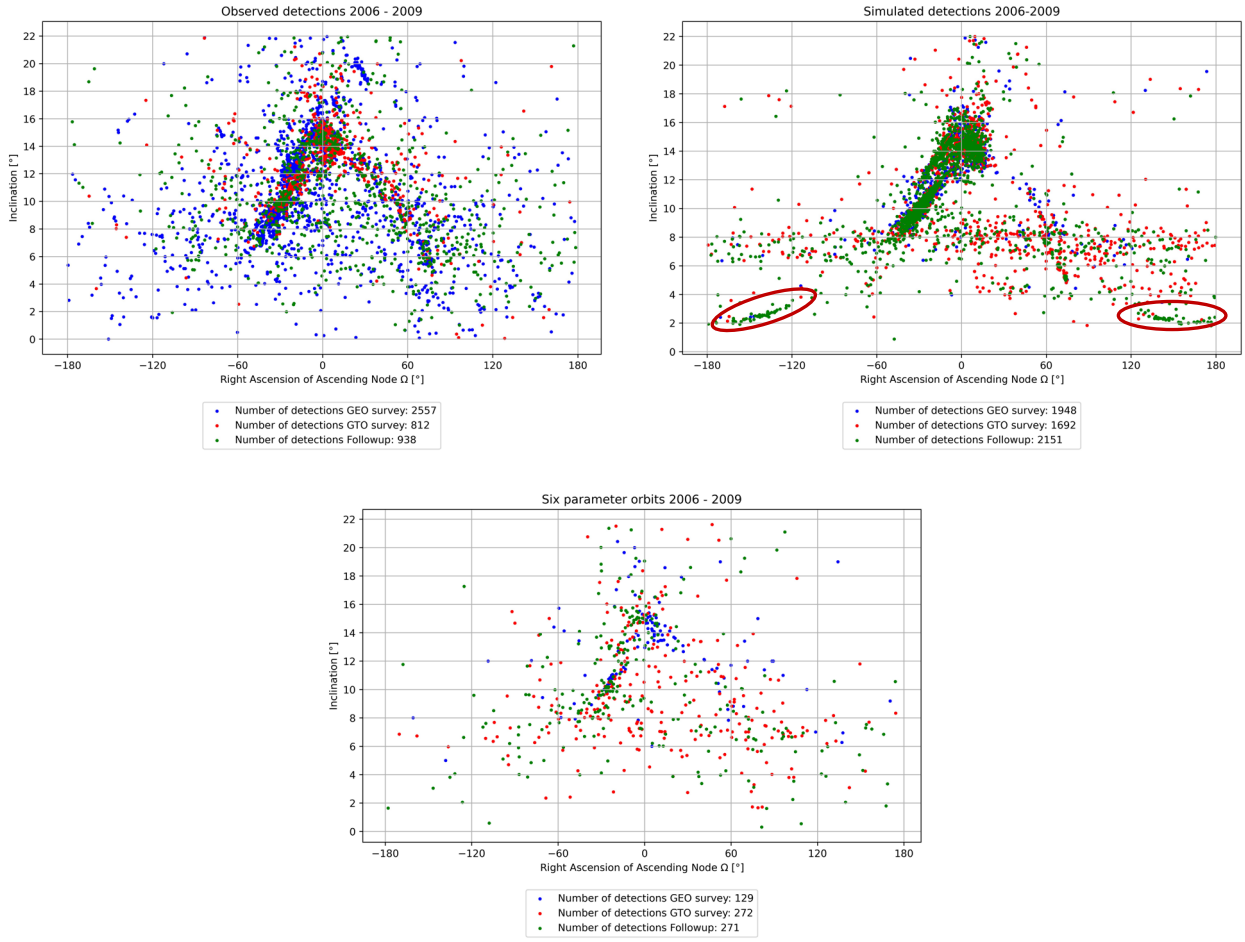

Figure 6: Orientation of the orbital planes of observed detections (top left), simulated detections (top right), and 6-parameter orbits (bottom) for the period 2006 to 2009.

Period 2010 to 2013 (Figure 7)

The situation is similar as in the previous period, the main simulated clusters along the “evolution path” are essentially seen in the detections, while the GTO population is not. In the simulation the previously unseen cluster has further evolved and is now at (80°/6°, 140°/2°). For the first time there might be some indication that some fragments from this cluster were detected.

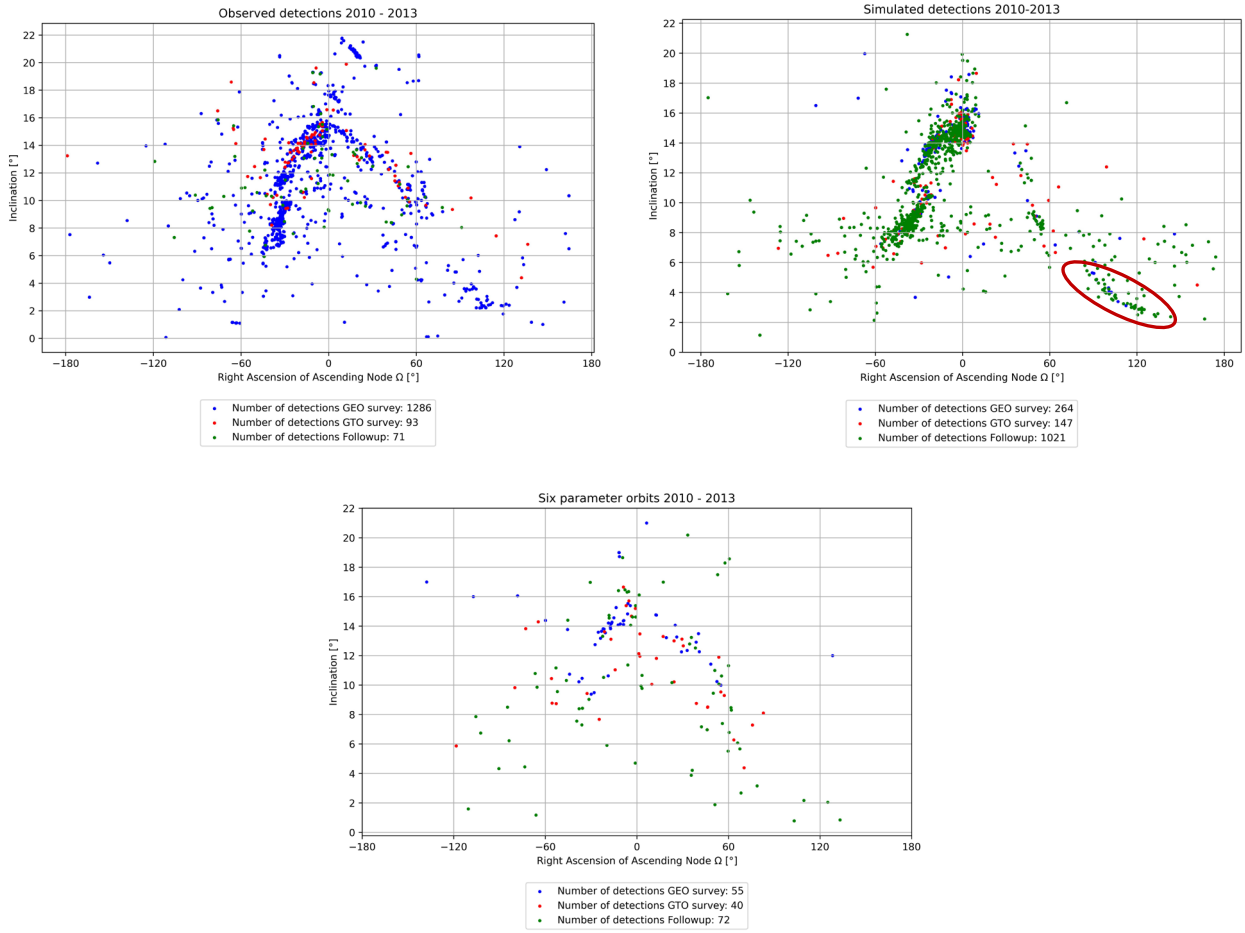

Figure 7: Orientation of the orbital planes of observed detections (top left), simulated detections (top right), and 6-parameter orbits (bottom) for the period 2010 to 2013.

Period 2014 to 2017 (Figure 8)

Observations (detections) from this period are very sparse which makes a direct comparison with the simulated observations difficult. Further analysis is needed to explain why the number of detections is much lower than predicted by the simulations.

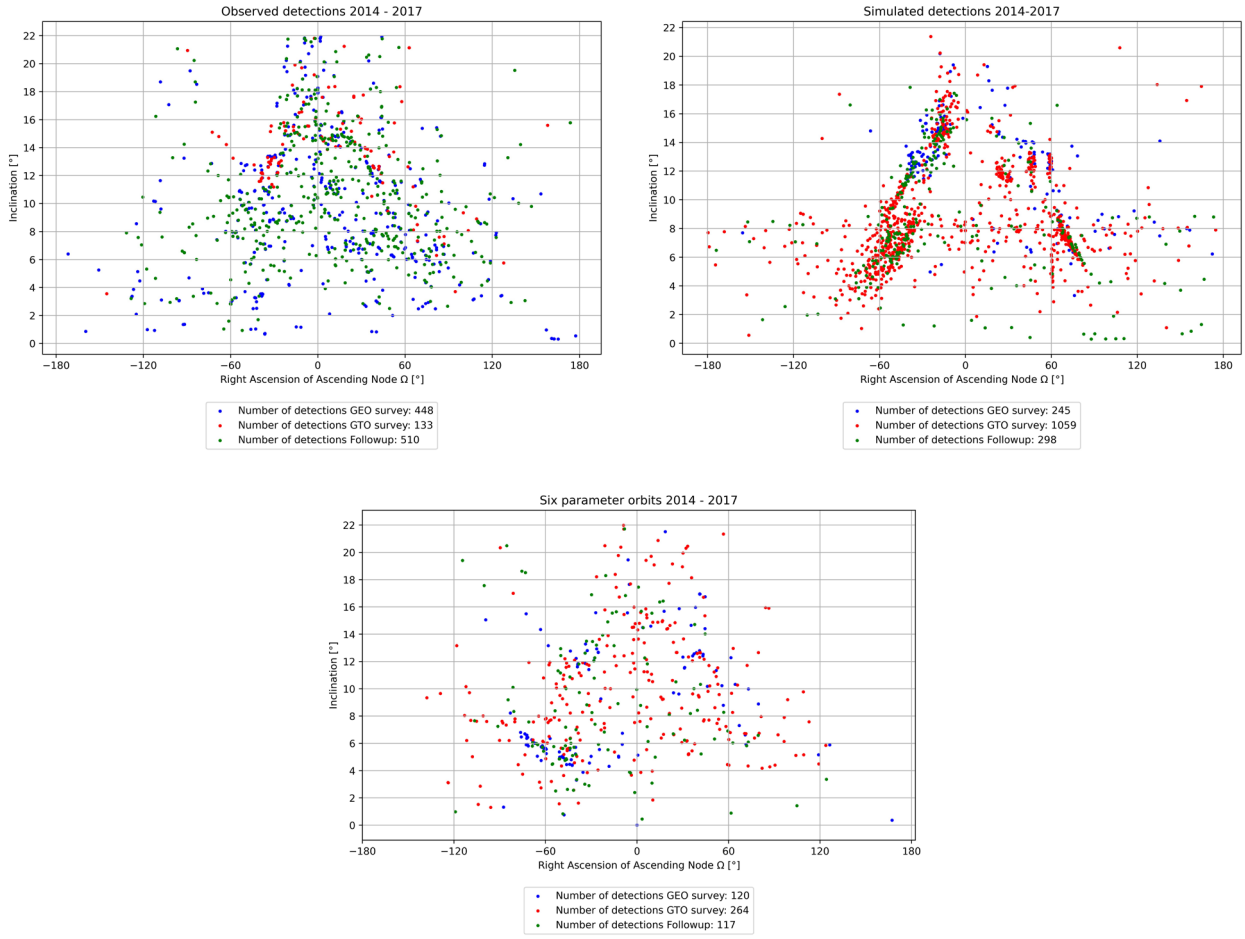

Figure 8: Orientation of the orbital planes of observed detections (top left), simulated detections (top right), and 6-parameter orbits (bottom) for the period 2014 to 2017.

Period 2019 to 2023 (Figure 9)

The number of detections from this period is again sufficient to allow a comparison with the simulated data. A new cluster in the region (10°/2°, 160°/2°) shows up in the simulated data but is not seen in the detections. Similarly, several clusters in the simulated observations in the region at (20°/16°, 90°/4°), and at (-70°/4°, -40°/8°), are not seen in the detections. These clusters seem to have been introduced into the MASTER population between 2013 and 2024. Two prominent clouds at (-110°/12°) and (-160°/10°) appear in the detections for the first time with no counterparts in the simulated observations.

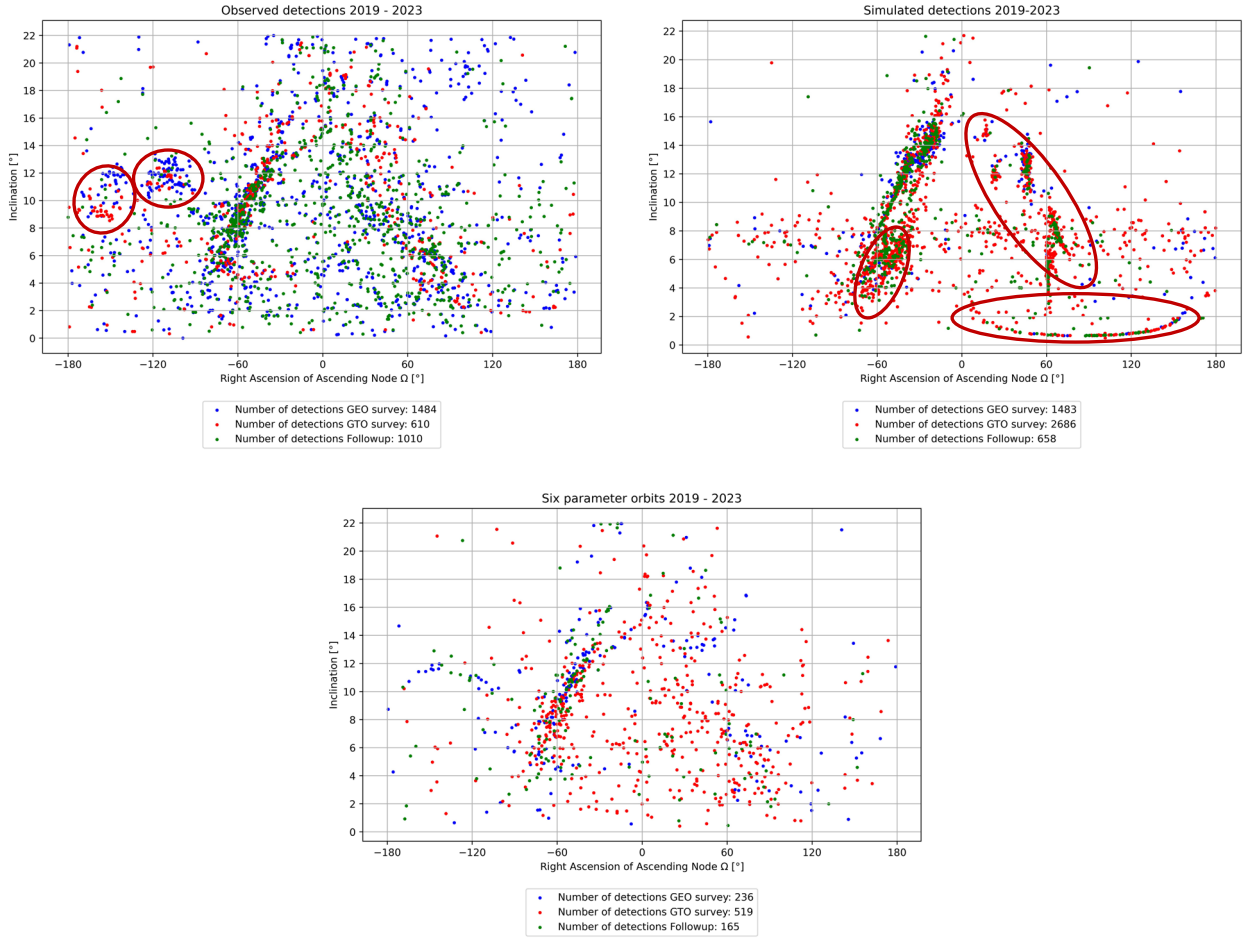

Figure 9: Orientation of the orbital planes of observed detections (top left), simulated detections (top right), and 6-parameter orbits (bottom) for the period 2019 to 2023.

5. SUMMARY

The results from 22 years of surveys observations to characterize the sub-catalogue population of space debris in high-altitude orbital regions were compared with simulated observations based on the MASTER model. The PROOF tool was used to simulate “detections” for the ESA 1-meter telescope at the OGS in Tenerife using the detailed list of pointing directions of over 730’000 survey observations. Orbital planes derived for about 14’500 observations of uncatalogued debris objects were compared with the simulated observations. The main conclusions are:

- The MASTER model predicts observations from orbitals planes with inclinations in the range from 4° to 8° and nodes evenly distributed in right ascension which are related to fragments attributed to Ariane GTO upper stages launched from Kourou. These objects were not seen in the observations. We conclude that either the MASTER model is overestimating this population or that the sensor model in PROOF is too optimistic for the GTO survey scenarios. This finding needs to be further analyzed.

- Throughout the entire period of 22 years the MASTER model is predicting observations of an old cluster of fragmentation debris which is not confirmed by the observations. Either this cluster does not exist, or its orbital planes evolved differently than predicted by MASTER. This could be the case if, e.g., most of the fragments in this cluster were high area-to-mass (HAMR) objects resulting in a dispersion of the orbital planes over time due to perturbations by solar radiation pressure.
- A new series of smaller debris clouds appears in the MASTER simulations from 2014 onwards which are not seen in the observations. These cluster located along the "evolution path" of the orbital plane indicating fragmentations of old objects.
- Observations of a prominent debris cloud at low inclination are predicted by the MASTER model for the recent years 2019-2023 but not confirmed by the real observations.
- Two new fragmentation clouds appear in the observations during the past 5 years indicated by clusters in the orbital plane space.

Further analysis is required to firmly exclude possible deficiencies in the PROOF sensor model and to further detail the discrepancies between the MASTER model predictions and the observations. The results confirm that the high-altitude debris population is very dynamic and that continuous observation campaigns are key to monitor this environment for new sources of space debris.

6. ACKNOWLEDGEMENTS

We would like to thank all the night observers and the technical staff at the ESA 1-meter telescope at the OGS and at the Swiss Optical Ground Station and Geodynamics Observatory Zimmerwald.

7. REFRENCES

[1] 'Space Debris', Report of the ESA Space Debris Working Group, ESA SP-1109, Paris, 1988.

[2] Flury, W., 'The Situation in the Geostationary Orbit', Workshop on Environmental Activities in Outer Space: State of the Law and Protection', Cologne, Germany, May 16-19, 1988.

[3] Flury, W., 'Collision Probability and Spacecraft Deposition in the Geostationary Orbit', Adv. Space Res., Vol. 11, No. 12, pp. 67-79, 1991.

[4] Lobb, D.R., 'Study on Optical Sensors for Space Debris Observations', Final Report, ESA ESOC Contract 9267/90/D/MD, 1992.

[5] Braun, V., Horstmann, A., Lemmens, S., Wiedemann, C., & Böttcher, L. (2021, April). Recent developments in space debris environment modelling, verification and validation with MASTER. In 8th European Conference on Space Debris (p. 18). ESA Space Debris Office Darmstadt, Germany.

[6] Schildknecht, T. (2007). Optical surveys for space debris. *The Astronomy and Astrophysics Review*, *14*, 41-111.

[7] Schildknecht, T., Musci, R., Ploner, M., Beutler, B., Flury, W., Kuusela, J., de Leon Cruz, J., de Fatima Dominguez Palmero, L. Optical observations of space debris in GEO and in highly-eccentric orbits. Adv. in Space Res., 34, 901–911, 2004.

[8] Schildknecht, T., R. Musci, T. Flohrer, Challenges Related to Discovery, Follow-Up, and Study of Small High Area-to-Mass Ratio Objects at GEO, proceedings of 2007 AMOS Technical Conference, pp 354–359, 12-16 September, Maui, Hawaii, USA, 2007.

[9] Schildknecht, T., Musci, R., M., Flury, W., Kuusela, J., de Leon Cruz, J., de Fatima Dominguez Palmero, L. Optical observations of space debris in high-altitude orbits, in: Danesy, D. (Ed.), Proceedings of the Fourth European Conference on Space Debris, ESA SP-587, ESA Publications Division, Noordwijk, The Netherlands, pp. 113–118, 2005.

[10] European Space Agency. *MASTER: Meteoroid and Space Debris Terrestrial Environment Reference*. Available at: https://sdup.esoc.esa.int/master/ (Accessed: 28 August 2024).

[11] Gelhaus, J., Flegel, S., & Wiedemann, C. (2011). *Final Report: Program for Radar and Optical Observation Forecasting*. Institute of Aerospace Systems (ILR), Technische Universität Braunschweig (TUBS). Contract Report No. 21705/08/D/HK. Document ID: M09/GEN-WP3200, Revision: 1.1. Braunschweig, Germany. Contact: Johannes Gelhaus. Main contractor: Institute of Aerospace Systems (ILR), Technische Universität Braunschweig (TUBS). Consultants: Dr. Michael Oswald, EADS Astrium Satellites; Dr. Sebastian Stabroth, EADS Astrium Satellites; Cenk Alagöz.

[12] Gelhaus, J., Flegel, S., & Krag, H. (2011). *Software User Manual*, PROOF 2009. Institute of Aerospace Systems (ILR), Technical University of Braunschweig (TUBS). Contract Report No. 21705/08/D/HK. Document ID: M09/PRO-SUM, Revision: 1.1. Braunschweig, Germany.

[13] Flegel, S., Oswald, M., Stabroth, S., & Alag, C. (2011). *Software User Manual*, MASTER 2009. Institute of Aerospace Systems (ILR), Technische Universität Braunschweig (TUBS). Contract Report No. RFQ No: 21705/D/HK. Proposal ID: M09/MAS-SUM, Revision: 1.1. Braunschweig, Germany. Contact: Sven Flegel.

[14] Flegel, S., Oswald, M., Stabroth, S., & Alag, C. (2011). *Final Report: Maintenance of the ESA MASTER Model*. Institute of Aerospace Systems (ILR), Technische Universität Braunschweig (TUBS). Contract Report No. RFQ No: 21705/08/D/HK. Proposal ID: M09/MAS-FR, Revision: 1.1. Braunschweig, Germany. Contact: Sven Flegel.

[15] Schildknecht, T., Flohrer, T., Musci, R., & Jehn, R. (2008). *Statistical Analysis of the ESA Optical Space Debris Surveys*. Acta Astronautica, 63(1-4), 119-127. doi: 10.1016/j.actaastro.2007.12.035. Pergamon, Oxford.